Biodiesel production from DK oils using Taguchi L9 techniques: characterization and thermogravimetric study of combustion characteristics

Ganesh Vijay More[1] · Y. V. Hanumantha Rao[1] · S. A. Kedar[2] · S. H. Gawande[3]

Abstract

Current environmental issues and depletion of natural petroleum resources demand alternative fuels for transportation. The present study deals with mixed dairy waste and Karanja oil (DK oils) biodiesel production using Taguchi L9 orthogonal array and characterization of the DK biodiesel blends to study its suitability as a renewable alternative fuel through gas chromatography, infrared spectroscopy, element analysis, physicochemical properties investigation, thermal behavior and combustion analysis using TG–DTG and TG–DSC techniques. Gas Chromatography was carried out to examine the quantification of fatty acid methyl esters, whereas infrared spectroscopy investigates the organic, inorganic, and polymeric contents with their vibrations in different molecular bonds. IS 1448 standard and elemental analysis is followed to examine the physicochemical properties of biodiesel and CHNSO percentage. Thermogravimetric analysis was followed to investigate the thermal behavior of the blends. Thermal analysis provides the information related to the stages of mass loss with temperature and mass loss percentage. The ignition temperature, burnout temperature, maximum combustion rate temperature, final decomposition temperature, ignition index, and comprehensive ignition index are the essential properties of fuel combustion analysis that are studied. Results indicate that the lower concentration of biodiesel in B20 blend provides a higher value of ignition index (1.67×10^{-4} to 3.86×10^{-4} min^{-1} °C^{-2}) and comprehensive ignition index (2.8×10^{-6} to 1.1×10^{-5} min^{-1} °C^{-3}) which provides better ignition performance during combustion.

Keywords DK biodiesel · GC–MS · FTIR · CHNSO · IS1448 standards · Thermogravimetric analysis

Introduction

For the past couple of decades, the energy crisis is being increased due to rapid consumption and insufficient supply of fossil fuels [1]. Diesel consumption is found to be much more than petrol consumption [2]. The biodiesel can bridge the gap of fossil fuel. The transport sector has a major contribution to the worlds' environmental pollution. It emits harmful pollutants such as smoke, carbon monoxide, carbon dioxide, unburnt hydrocarbons, nitrogen oxides, and particulate matter. Biodiesel has several advantages (like safe storage and transportation, improving combustion efficiency, and minimizing the exhaust gas harmful emissions) and few drawbacks (like more NOx emission and high viscosity). The high flash point temperature of biodiesel makes it safer for storage, as well as transport, when compared to gasoline fuel [3]. More than 350 types of feedstocks are identified to produce biodiesel, which is categorized into first, second, and third-generation feedstocks [4].

In India, biodiesel production from first-generation feedstocks is economically unviable, whereas a variety of second-generation [5, 6] (like Neem, Tobacco, Mahua, Rubber, Jatropha, Karanja, Castor, Tung, Jojoba, etc.) and third-generation feedstocks [7] (waste cooking oils, chicken fat, animal fat, fish oil, algae, and dairy waste, etc.) are widely available and economically viable. Indian government encourages nonedible products for producing biodiesel.

✉ Ganesh Vijay More
  ganeshmr135@gmail.com

1 Department of Mechanical Engineering, Koneru Lakshmaiah Education Foundation, Deemed to be University, Vaddeswaram, India

2 Department of Mechanical Engineering, MKSSS's Cummins College of Engineering for Women Pune, Pune, India

3 Department of Mechanical Engineering, M.E.S. College of Engineering, S.P. Pune University, Pune, India

Dairy factories are producing milk-related products like milk powder, cheese, paneer, ghee, ice-cream, etc. Various kinds of equipment are used for different processes. While cleaning the washed-out, considerable amount of residual fats, ghee, butter, etc., are in the sewage processing section in sustainable quantities as dairy waste scum. Large dairy industries are found difficult in disposing of the waste, which consists of unsolicited materials, proteins, lipids, fat, etc. This dairy waste increases environmental pollution [8]. Watkins and Nash [9] have proposed the possible reuse of dairy waste. The second-generation feedstock consists of nonedible oils like jatropha, neem, castor, Karanja, etc. Jatropha requires less water and manure. It grows in a short period and yields more seeds. Jatropha seeds have more oil content. However, it requires proper agricultural land [10]. The Karanja possesses the qualities of Jatropha. Karanja trees can grow on the sides of streets and channels.

Quality of biodiesel has influenced by several factors like a strategy for feedstock preparation, biodiesel synthesis method, chemical composition, and biodiesel purification. For the evaluation of the quality of biodiesel, significant standards have found out. For all biodiesels, it is essential to satisfy the requirement of standards of biodiesel authorized by the American Society for Testing and Materials (ASTM D6751)/European Standard (EN 14214)/Indian standard (IS 1448). These standards provide a baseline for testing biodiesels and suggest the range for several physicochemical properties of the fuel, which is useful for diesel engines [11]. In the sense of diesel engine, the important physicochemical properties of the fuel are kinematic viscosity, density, cetane number, acid value, calorific value, flash point, fire point, cloud point, pour point, and element analysis (CHNSO analysis) [12, 13]. The quality of biodiesel affects the performance and emission characteristics of the engine [14, 15]. Gas chromatography–mass spectroscopy (GC–MS) technique is useful for the quantification of fatty acid methyl esters (FAME) and identifies the presence of chemical components in biodiesel. Biodiesel has a combination of both saturated and unsaturated (polyunsaturated and monounsaturated) fatty acids, which represent the quality of biodiesel during combustion [16]. The infrared spectroscopy technique is important to investigate the organic, inorganic, and polymeric contents in addition to their vibrations in different molecular bonds [17, 18]. Thermogravimetric (TG), derivative thermogravimetric (DTG), and differential scanning calorimetry analysis (DSC) are useful techniques to study the thermal behavior of fuel. The thermal analysis of fuel provides significant information related to combustion behavior and thermal characteristics, which include ignition temperature, burnout temperature, enthalpy, entropy, activation energy, phase transition, heat capacity, and Gibbs free energy [19]. This information is of great importance for combustion studies. According to the feedstock of biodiesel,

the blends present different combustion characteristics and thermodynamic properties. TG is a technique in which the mass of a substance is measured as a function of temperature and time. DSC is a technique in which the difference in energy input into a substance and the reference material is measured as a function of temperature or time. In DSC, the substance and reference material are subjected to a controlled temperature program. TG analysis is useful to study temperature stability, mass changes, decomposition, oxidation behavior, and kinetic analysis. DSC study is important to investigate transition behavior, specific heat, melting behavior, glass transitions, degree of crystallization, oxidative stability. This thermal analyzer performs a simultaneous TG–DSC and TG–DTG measurement on the sample. Dweck and Sampaio [20] investigated the thermal decomposition of different vegetable oils (corn oil, olive oil, and sunflower oil) using TG–DTA analysis. Candeia et al. [21] studied the rheological and thermal behavior of soybean biodiesel blends. They explained that during the mass loss step (TG curve), combustion and evaporation occur in between methyl esters, as well as olefins, naphthenes, paraffin, and aromatics, with a C12-18 carbon. Santos et al. [22] studied the calorimetric and thermogravimetric evaluation of babassu biodiesel. They concluded that the different atmosphere did not affect significantly the evaporation of biodiesel. Moreover, the result reveals that the biodiesel shows three mass loss steps during thermal analysis. Souza et al. [23] investigated the thermal and kinetic behavior of cotton oil biodiesel. In this study, they investigated mass loss steps with decomposition temperature and different kinetic parameters of cotton oil, as well as biodiesel. Oliveira and Dweck [24] studied the oxidation stability of biodiesel blends using TG and DTA techniques. They concluded that the increased percentage of biodiesel in blend promoted enhanced thermal and oxidation instability resulting more oxidation stages in liquid form. Meireles et al. [25] investigated thermo-oxidative stability and physicochemical characteristics of catole coconut oil. The cold press oil resulted 2.48 mg KOH g^{-1} acid value, 0.14 meq peroxide kg^{-1} peroxide value, and 253 mg KOH g^{-1} saponification value. The thermogravimetric profile of oil remained stable up to 240 °C. Cortes et al. [26] investigated the degrees of oil conversion into biodiesel applying quasi-isothermal thermogravimetry. TG curves clearly distinguished between the mass losses caused by ester volatilization and that resulting from oil thermal decomposition. Oliveira et al. [27] applied the mixed oxide for biodiesel production from cotton oil and monitoring by TGA. The catalyst 0.25Ca–0.75Ti (calcined at 800 °C) produced highest 92.2% yield.

In the overview of the ongoing literature reviewed, it is seen that no one worked on DK biodiesel and its characterization. Hence, this study deals with biodiesel production from equally mixed dairy waste and Karanja (DK) oil.

It presents the biodiesel preparation using Taguchi's L9 orthogonal array and characterization of the DK biodiesel blends to study its suitability as renewable alternative fuel through gas chromatography, infrared spectroscopy, element analysis, physicochemical properties investigation, thermal behavior and combustion analysis using TG–DTG and TG–DSC techniques. Using standard methods, physicochemical properties of biodiesel were determined. Also, a comparison of the properties with other biodiesels was presented for additional interest.

Material and method

Materials

Dairy waste was collected from the dairy industry and purified. Karanja seeds were collected from the agricultural field and oil was extracted through cold press machines. The chemicals procured are methanol alcohol (AR grade, 99% pure), sulfuric acid (H_2SO_4) (LR grade, 99% pure), and potassium hydroxide (KOH) (99% pure).

Feedstock preparation and property evaluation

The white color semisolid dairy waste scum is heated for purification prior to oil extraction. Karanja seeds are dried to remove the moisture content and extracted oil through a cold press machine. 28% of oil yield is achieved during extraction. The dairy waste and Karanja seed oils are equally mixed (DK oils) for biodiesel production. To achieve a homogeneous mixture, a magnetic stirrer (650 rpm) is used with a heating plate (100 °C) for 90 min. Investigations are made on the characterization of dairy waste scum, Karanja seed oil and converted equally mixed oils into FAME. The physicochemical properties of the prepared samples have been tested as per IS standards at Hi-Tech Laboratory, India. Characterization of dairy waste indicates 70.52% free fatty acid (FFA) content which is very high when compared to that

of other feedstocks (varying below 45%). High quantities of FFA content increase oil corrosiveness (acidity), powerlessness to oxidation, accelerate debasement and restrain soluble catalyzed transesterification [28]. FFA content for Karanja oil is found to be 4.96%. For equally mixed dairy waste and Karanja oil, the FFA content is found to be 37.64% which seems to be high. Two-step transesterification procedure has to be adopted to control the FFA content. The humidity of Karanja oil, dairy waste scum, and prepared feedstock (hybrid oil) was 0.91%, 1.2%, and 1.1% respectively. The acid value of Karanja oil is 15.2 mg KOH g^{-1} of oil, which is less when compared to that of dairy waste (70.52 mg KOH g^{-1}). DK oil sample indicates the acid value of 37.64 mg KOH g^{-1}. The calorific value of Karanja oil, Dairy waste scum, and DK sample was 37.53 MJ kg^{-1}, 36.99 MJ kg^{-1}, and 37.31 MJ kg^{-1}, respectively. The calorific value of all oil samples was nearly the same. All three oil samples showed the same density as 903.9 kg m^{-3}. The Karanja seed oil possesses a high flash point (428 °C) when compared to waste dairy scum (275 °C) and DK oil (287 °C). The viscosity of all oil samples is close to 38 mm^2 s^{-1}. Table 1 gives the physicochemical properties of feedstock oils.

Production of DK biodiesel

The transesterification process converts triglycerides into alkyl esters. The whole process depends on the FFA content of the feedstock oil. If FFA content is less than 2%, then a single-stage transesterification procedure is sufficient to convert the triglycerides (oil) into FAME. If FFA content is more than 2%, then both esterification and transesterification processes are required to convert the triglycerides (oil) into FAME. The 34.64% FFA content of DK oil is found to be high. A two-step transesterification process is adopted to reduce the FFA content. The yield of FAME depends on molar ratio, catalyst concentration, reaction temperature, and reaction time.

A 50 mL batch size (oil sample) is used for the esterification process. The oil is preheated to 80 °C. Methanol

Table 1 Physicochemical properties of feedstock oils

Oil properties	Unit	Karanja oil (KO)	Dairy waste (DW)	Equally mixed DK Oil
Color	–	Dark brown	White	Brown
Density (40 °C)	Kg m^{-3}	903.9	903.9	903.9
Viscosity (40 °C)	$mm^2 s^{-1}$	37.48	38.78	37.92
FFA content	%	4.96	70.52	37.64
Moisture	%	0.91	1.2	1.1
Acid value	mg KOH g^{-1}	15.2	70.52	37.64
Calorific value	MJ kg^{-1}	37.53	36.99	37.31
Flash point	°C	428	275	287

is selected as alcohol [29] and sulfuric acid (H$_2$SO$_4$) as a catalyst for esterification [30]. The methanol and sulfuric acid are mixed prior to adding the preheated oil sample. The esterification reaction was accomplished with a specified process parameter (6:1 molar ratio, 1mass% catalyst concentration, 60 °C reaction temperature, 60-min reaction time). After the esterification reaction, the phase separation is carried out with a separating funnel and washing of FAME with distilled water. Figure 1 shows the DK oil sample and its phase separation after transesterification reaction.

A 50 mL batch size (esterified oil sample) is used for the transesterification process. The transesterification with potassium hydroxide (KOH) as a catalyst produced better results (see Fig. 1). The transesterification reaction is accomplished with different molar ratios (4.5:1, 6:1, and 7.5:1), catalyst concentrations (0.7, 1, 1.3 mass%), reaction temperature (50, 60, and 70 °C) and reaction time (45, 60, 75 min). A combination of these process parameters is preferred while producing biodiesel. The purified FAME is heated at 100 °C to minimize the moisture content. The %FAME yield is evaluated from Eq. (1) [31]. FAME analysis has been carried out as per IS 1448 standard.

$$\text{FAME Yield}(\%) = \frac{\text{Mass of FAME}}{\text{Mass of hybrid oil in experimentation}} \times 100 \tag{1}$$

Experiments have been carried out based on Taguchi's L_9 orthogonal array and evaluated the %FAME yield for the specified process parameters. In the plan of experiments, three levels are set for each parameter. For ease of reference, these four parameters are designated by A, B, C, and D, respectively. Table 2 presents the input parameters and

Table 2 Input parameters and levels

Parameters	Designation	Levels		
		1	2	3
Molar ratio	A	4.5:1	6:1	7.5:1
Catalyst concentration (mass%)	B	0.7	1	1.3
Reaction temperature (°C)	C	50	60	70
Reaction time (min.)	D	45	60	75

their levels. Table 3 gives %FAME yield for the set of input process parameters as per the Taguchi's.

Analysis of variance (ANOVA)

Taguchi method [32] is a systematic statistical approach successfully used in obtaining optimal solutions for many engineering/industrial problems. ANOVA is performed on the %FAME yield data of Table 3, and the results are presented in Table 4. It is noted that reaction time (D) has maximum %Contribution on %FAME yield with 53.21% and other parameters like molar ratio (A), catalyst concentration (B), reaction temperature (C) on the %FAME are 33.45%, 9.4%, and 3.94%, respectively. From the ANOVA Table 4, the maximum value of %FAME yield is obtained for a set of process parameters $A_2B_2C_2D_3$.

The additive law [33] in Eq. (2) is used to estimate the %FAME yield (ϕ) for each test run in Table 3.

$$\widehat{\phi} = \phi_{\text{mean}} + \sum_{i=1}^{n_p} \left(\phi_i - \phi_{\text{mean}} \right) \tag{2}$$

Fig. 1 DK oil sample and its phase separation

Table 3 % FAME yield as per Taguchi's

Level for input parameters				%FAME yield		
A	B	C	D	Test	Additive law in Eq. (2)	Empirical relation (3)
1	1	1	1	65	65	65
1	2	2	2	85	85	85
1	3	3	3	81	81	81
2	1	2	3	91	91	91
2	2	3	1	84	84	84
2	3	1	2	88	88	88
3	1	3	2	84	84	84
3	2	1	3	87	87	87
3	3	2	1	74	74	74

Table 4 ANOVA results on %FAME yield

Parameters	1-mean	2-mean	3-mean	Sum of squares	% Contribution
A	77	87.67	81.67	171.56	33.45
B	80	85.33	81	48.22	9.40
C	80	83.33	83	20.22	3.94
D	74.33	85.67	86.33	272.89	53.21

Here, $\widehat{\phi}$ is the estimated %FAME yield; $\phi_{mean} = 82.11$ is the overall mean of ϕ; ϕ_i is the mean of ϕ at the specified level for the parameters (i), and $n_p = 4$ is the number of parameters. For these optimal parameters (viz., molar ratio, $A_2 = 6{:}1$; Catalyst concentration, $B_2 = 1$ mass%; reaction temperature, $C_2 = 60$ °C; and reaction time, $D_3 = 75$ min.), Eq. (2) estimates %FAME yield as

where $\emptyset_A(x) = -8.33x^2 + 2.33x + 87.67$; $\emptyset_B(x) = -4.83x^2 + 0.5x + 85.33$; $\emptyset_C(x) = -1.83x^2 + 1.5x + 83.33$; $\emptyset_D(x) = -5.33x^2 + 6x + 85.67$; and $\emptyset_{mean} = 82.11$

Estimates of %FAME yield from the developed empirical relation (3) for the specified values of A, B, C, and D corresponding to the levels in Table 3 are also in good agreement with the test results. The advantage of empirical relation (3) is to estimate the %FAME yield for any set of process parameters within the set levels. Estimates using the empirical relation (3) are reasonably in good agreement with the test results. Several tests are performed on these optimal process parameters, confirmation test result gives %FAME yield as 94%.

Blend preparation and characterization

The DK biodiesel is blended with diesel in different ratios (B20, B30, B40, B100) (see Fig. 2). The gas chromato-

$$\begin{aligned}
\widehat{\phi} &= \phi_{mean} + \left(\phi_{A2} - \phi_{mean}\right) + \left(\phi_{B2} - \phi_{mean}\right) + \left(\phi_{C2} - \phi_{mean}\right) + \left(\phi_{D3} - \phi_{mean}\right) \\
&= 82.11 + (87.67 - 82.11) + (85.33 - 82.11) + (83.33 - 82.11) + (86.33 - 82.11) \\
&= 96.33
\end{aligned}$$

The estimated %FAME yield for the optimal processing parameters is close to the confirmation test results of 94–96%. To examine the adequacy of the additive law in Eq. (2), %FAME yield values estimated for the set of process parameters in Table 3 are found to be in good agreement with test results.

Based on the ANOVA results, the empirical relation is developed for a percentage of FAME yield in terms of molar ratio (A), catalyst concentration (B), Reaction temperature (C), reaction time (D) which is as follows,

graph is used for analyzing the compositions of different fatty acid esters with high-resolution mass spectrometer (GC-HRMS) using Agilent 7890 with an FID detector, headspace injector, and combipal autosample. The infrared spectroscopy techniques are used to investigate the organic, inorganic, and polymeric contents with vibrations in different molecular bonds. The element analysis is performed to record the percentage of carbon, hydrogen, nitrogen, sulfur, and oxygen (CHNSO) in biodiesel using the Flash EA 1112 series with an autosampler, combustion
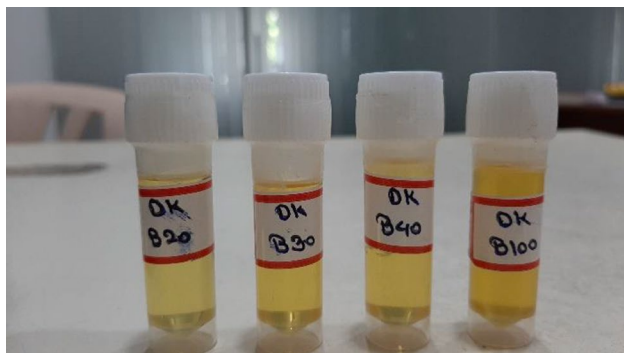
$$\%\text{FAME Yield} = \emptyset_A\left(\frac{A-6}{1.5}\right) + \emptyset_B\left(\frac{B-1}{0.3}\right) + \emptyset_C\left(\frac{C-60}{10}\right) + \emptyset_D\left(\frac{D-60}{15}\right) - 3\emptyset_{mean} \tag{3}$$

Fig. 2 Biodiesel blends

reactor, chromatographic column, and T. C. D. detector. The biodiesel sample is analyzed by the thermal analyzer (NETZSCH STA 449 F3 Jupiter) to record the TG, DTG, DSC results. For all biodiesels, it is essential to satisfy the requirement of standards of biodiesel authorized by the American Society for Testing and Materials (ASTM D6751)/ European Standard (EN 14,214)/ Indian standard (IS 1448). These standards provide a baseline for testing the biodiesels and suggest the range for several physicochemical properties of the fuel, which is useful for diesel engines. The physicochemical properties affect the engine performance, emission, and durability, as well as fuel efficiency. Using standard methods, physicochemical properties of blends were determined. Also, a comparison of the properties with standards such as ASTM D6751 and EN 14214 was presented for additional interest.

Combustion characteristics

Several techniques have been proposed to investigate the ignition (T_i) and burnout (T_b) temperature of fuel through thermal analysis. The present study deals with two different techniques such as conversion method [34, 35], intersection method [36–38], 1%/min conversion rate method [34, 39]. The intersection method follows the TG–DTG tangent technique to investigate ignition temperature, burnout temperature, and maximum combustion rate temperature (T_m). The conversion method investigates the ignition temperature at 10% conversion and burnout temperature at 95%. The 1% min^{-1} conversion rate method examines the ignition temperature at which the combustion rate achieves 1 mass% min^{-1} conversion rate, while burnout temperature investigates at which the burning rate descends to 1 mass% min^{-1}. The burnout temperature also investigated using two other methods as 0.1% min^{-1} conversion rate method [34, 39] and at 99% mass reduction method [34, 35]. The 0.1% min^{-1} conversion rate method examines the burnout temperature at which the burning rate falls to 0.1 mass% min^{-1}. The second

method examines the burnout temperature, where the fuel conversion reaches 99%.

The ignition temperature is examined at a point at which the thermal acceleration curve starts to change from the initial temperature. The portion between ignition point and primary the inflection point is denominated as the ignition zone, while the portion between the primary to secondary inflection point is denominated as the burning zone [40]. The final stage in the thermal acceleration curve is the burnout zone, the temperature between the second inflection point and the final value, and the final temperature is the burnout temperature.

Ignition index (Di) and comprehensive performance index (Dc) were investigated to analyze the data of the ignition performance of the fuel, which indicates how slow or fast fuel ignites.

$$Di = \frac{DTG_{max}}{T_i\,T_b} \tag{4}$$

$$Dc = \frac{DTG_{max}\,DTG_{mean}}{T_i^2\,T_b} \tag{5}$$

where DTG_{max}: maximum mass loss rate; DTG_{mean}: mean mass loss rate.

Results and discussion

This paper deals with the characterization of Karanja oil, dairy waste, and DK oil. Characterization of DK biodiesel is performed to examine its suitability for CI engines. The FFA content of the DK oil is above 2%, the two-step transesterification process is carried out. A maximum of 94% FAME recovery is obtained with methanol as alcohol, sulfuric acid (H_2SO_4) as a catalyst during esterification, potassium hydroxide (KOH) as a catalyst during transesterification along with 6:1 molar ratio, 1mass% catalyst concentration, 60 °C reaction temperature, 75-min reaction time.

Gas chromatography–mass spectroscopy

The DK biodiesel sample is analyzed by gas chromatograph with high-resolution mass spectrometer (GC-HRMS) (Agilent 7890 with FID detector, head space injector, and combipal autosampler) at SAIF IIT Bombay. Table 5 shows the presence of various fatty acids with respect to their formula, retention time, fatty acid molecular structure. Figure 3 reveals the presence of fatty acids as apex identified by comparing the mass spectrum of individual esters. It clearly showed that the DK biodiesel contained mainly, methyl tetradecanoate; hexadecanoic, acid methyl ester; 9,12-octadecadienoyl chloride, (z, z)-; 9-octadecenoic acid

Table 5 Fatty acid methyl esters in DK biodiesel

Ester compounds	Fatty acids	Chemical formula	Retention time/min.
Methyl tetradecanoate	Myristic	$C_{15}H_{30}O_2$	21.51
Hexadecanoic acid, methyl ester	Palmitic	$C_{17}H_{34}O_2$	25.78
9,12-Octadecadienoyl chloride, (Z, Z)-	Linoelaidic	$C_{18}H_{31}ClO$	38.45
9-Octadecenoic acid (Z)-, methyl ester	Oleic	$C_{19}H_{36}O_2$	30.09
Octadecenoic acid, methyl ester	Stearic	$C_{19}H_{38}O_2$	30.53
Hexadecanoic acid, 2-hydroxy-(hydroxymethyl)ethyl ester	Palmitic	$C_{19}H_{38}O_4$	36.43

Fig. 3 Fatty acid composition of DK biodiesel
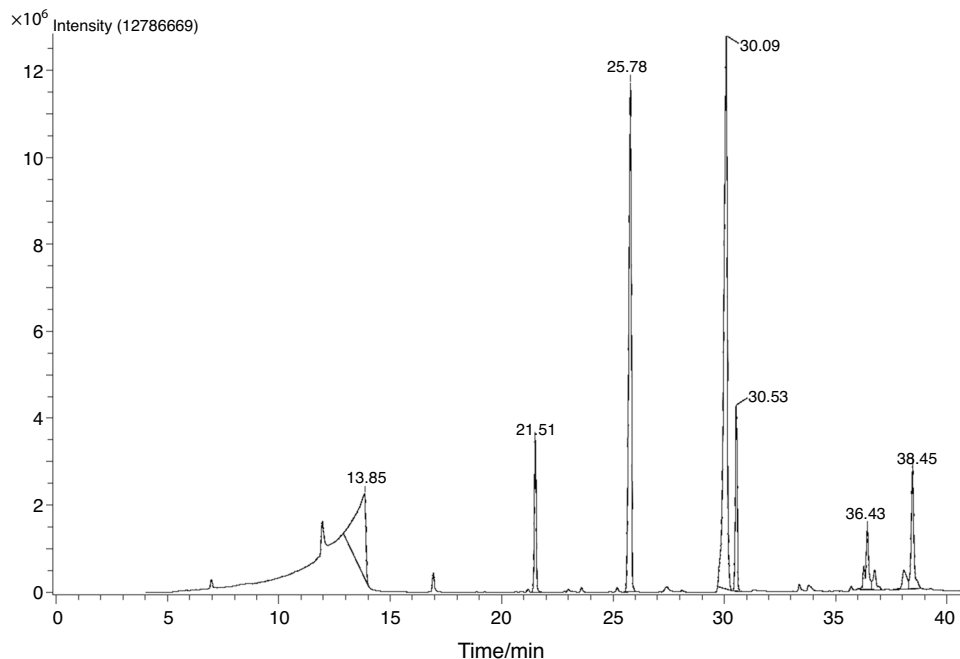
(z)-, methyl ester; octadecenoic acid, methyl ester; hexadecanoic acid, 2-hydroxy-(hydroxymethyl) ethyl ester. If the GC–MS profile of biodiesel represents a combination of saturated, polyunsaturated, and monounsaturated fatty acids, it is considered as good of quality biodiesel according to ASTM D6751-07 standard [41]. The biodiesel profile represents the presence of oleic acid. This is good for the balance of fuel in terms of oxidative stability, ignition quality, and viscosity [42].

Fourier transform infrared spectroscopy

The different blends (B20, B30, B40, and B100) of biodiesels and diesel fuel have been analyzed through Fourier transform infrared spectroscopy (FTIR). Table 6 and Figs. 4–8 provide the FTIR results of the blends. The symmetric and asymmetric stretching vibrations of alkane C–H stretching in the CH group are illustrated only in diesel. The symmetric and asymmetric stretching vibrations of alkane C–H stretching in the CH_2 and CH_3 groups are illustrated in all tested blends. The stretching vibration due to the carbonyl group (–C=O) is illustrated in all tested blends except diesel. The bending vibrations of CH_2 and CH_3 groups are illustrated in all tested blends. The symmetric and anti-symmetric stretching vibrations of the C–O–C group are illustrated in high concentrated biodiesel blends B40 and B100. The CH_2 twisting and CH wagging vibrations of alkane C–H in vinyl hydrocarbon compounds and –CH=CH_2 functional group are illustrated in diesel, B30 and B100 blends.

Element analysis

The element analysis provides the percentage composition of carbon, hydrogen, nitrogen, sulfur, and oxygen (CHNSO) in biodiesel. The biodiesel sample is analyzed by CHNS(O) analyzer adopting the "Dumas Method." It carries the entire and momentary oxidation of the sample by "flash combustion." Figure 9 reveals the presence of CHNS elements. The

Table 6 Infrared spectroscopy vibration

Blends	Types of vibrations with wavenumber/cm^{-1} and strength							
	Symmetric and asymmetric stretching vibrations of alkane C–H stretching			Stretching vibration due to carbonyl	Bending vibration		Symmetric and anti-symmetric stretching vibrations	Twisting and wagging due to Alkane C–H
Group →	CH	CH$_2$	CH$_3$	–C=0	CH$_2$	CH$_3$	C–O–C	–CH=CH$_2$
Diesel (Fig. 4)	Strong (2968.98)	Strong (2935.69)	Strong (2870.64)	–	Medium (1466.35)	Short (1382.10)	–	Short (694.97)
B20 (Fig. 5)	–	Strong (2921.56)	Short (2853.59)	Short (1745.72)	Medium (1458.83)	–	–	–
B30 (Fig. 6)	–	Strong (2921.80)	Short (2853.46)	Short (1745.41)	Medium (1462.39)	Short (1376.18)	–	Short (619.32)
B40 (Fig. 7)	–	Strong (2921.83)	Short (2854.10)	Short (1744.14)	Medium (1460.84)	Short (1376)	Short (1164.79)	–
B100 (Fig. 8)	–	Strong (2922.71)	Strong (2853.28)	Strong (1741.56)	Strong (1461.30)	Short (1371.62)	Medium (1166.73)	Short (654.89)
Diesel [1]	–	Strong (2924)	Strong (2855)	–	Medium (1462)	Short (1378)	–	Short (725)
Pequi Bio-diesel [17]	Medium (3008)	Strong (2928)	Strong (2853)	Strong (1741)	Medium (1434)	Short (1365)	Short (1100)	Short (722)
Rubber Bio-diesel [43]	Medium (3012)	Strong (2920)	Strong (2855)	Strong (1743)	Medium (1460, 1440)	Medium (1368)	Medium (~ 1300–1000)	Short (720)
Peanut Bio-diesel [44]	–	Strong (2924)	Strong (2850)	Strong (1745)	Medium (1465)	Short (1377)	Medium (1170)	Strong (678)

Fig. 4 Infrared spectroscopy of diesel FTIR
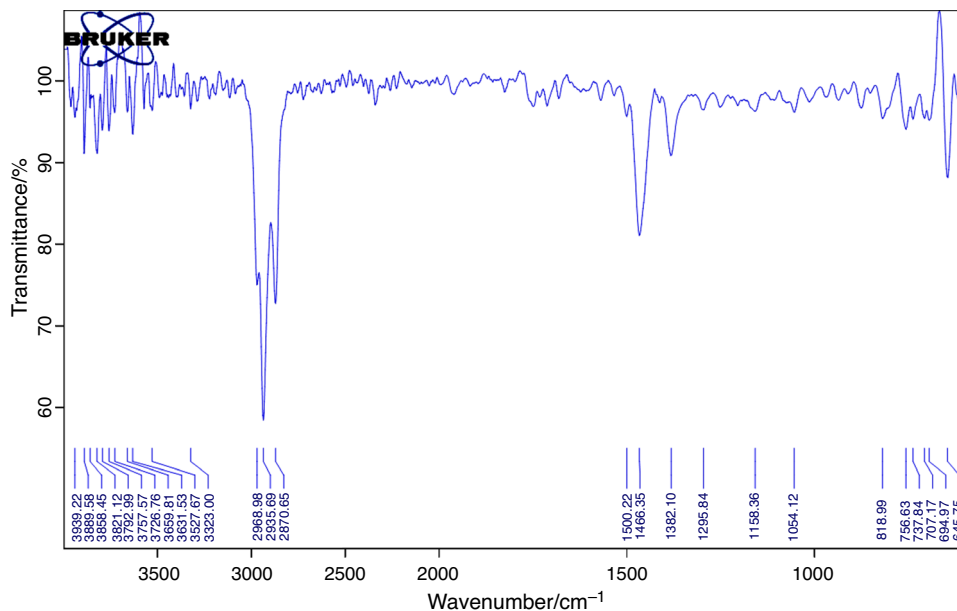
DK sample possesses 74.29% carbon, and 1.566% nitrogen with 1.025 and 0.742-min retention time, respectively. The ASTM D6751 standard suggests a maximum of 77% carbon in biodiesel. The cetane number of biodiesels is dependent on the presence of carbon content in fuel. The higher carbon content improves the cetane number [45]. DK biodiesel has 12.378% hydrogen with 3.308-min retention time. The ASTM D6751 standards recommend a maximum of 12% hydrogen in biodiesel. At present, the emission acts stringently restrict the sulfur content in the fuel because the

Fig. 5 Infrared spectroscopy of B20 FTIR
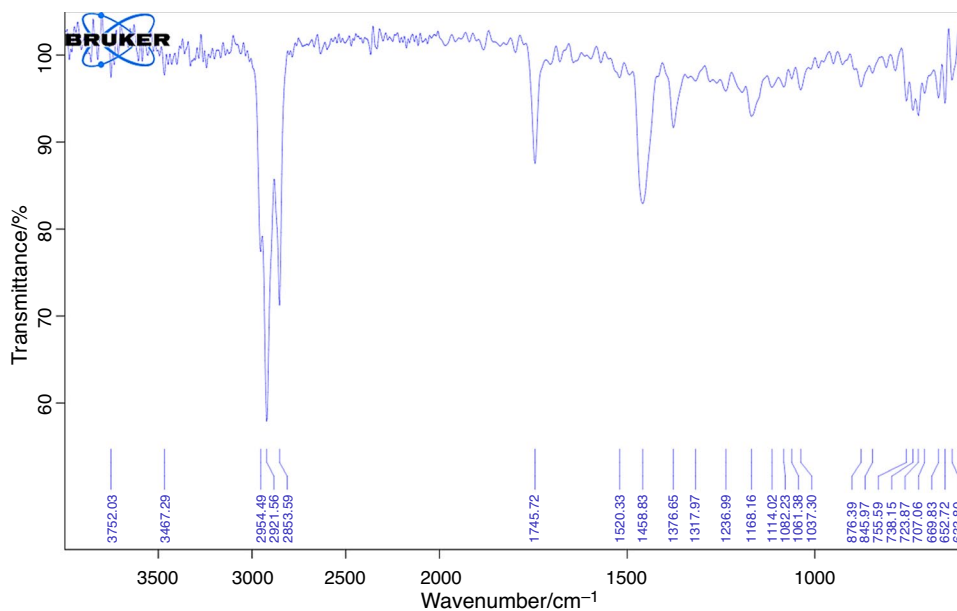
Fig. 6 Infrared spectroscopy of B30 FTIR
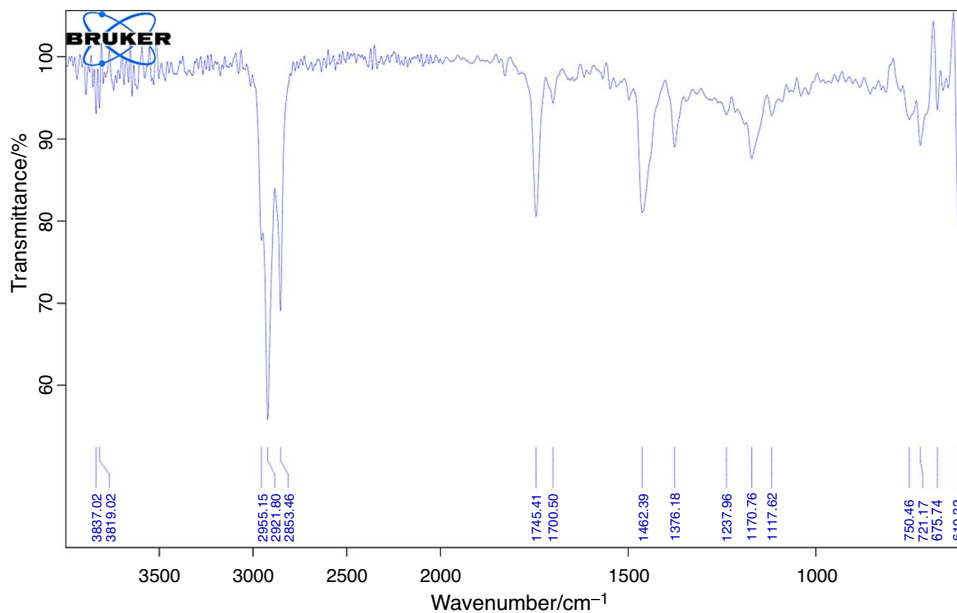
emission of sulfur oxide is mainly responsible for acid rain. In the present work, used biodiesel is sulfur-free. It automatically takes away the sulfur oxide emission. It also meets the requirement of emission acts. DK biodiesel has 11.76% oxygen. As per ASTM D6751, the biodiesel is required to maintain 11% oxygen content. The oxygen content in biodiesel assists the combustion at high temperatures, which provides less CO and CO_2 emission [42]. The more amount of oxygen content motivates the fuel blend for oxidation at the time of combustion which lead to less emission of HC, CO, and PM [41]. Also, the higher cetane number and more amount of oxygen content would minimize the ignition delay period and parallelly accelerate the burning rate in the

premixed combustion phase [41]. The carbon, hydrogen, and oxygen contents of DK biodiesel have met the standards specifications.

Thermogravimetric analysis

The biodiesel sample is analyzed by the thermal analyzer (NETZSCH STA 449 F3 Jupiter) at SAIF IIT, Madras, to record the TG, DTG, DSC results. Figures 10–13 provide the results of TG–DTG techniques for different blends. According to TG and DTG curve at B20 blend, two mass loss steps occur. The first mass loss occurs between 65 and 260 °C, during this 86.04% mass burnt, while second mass loss

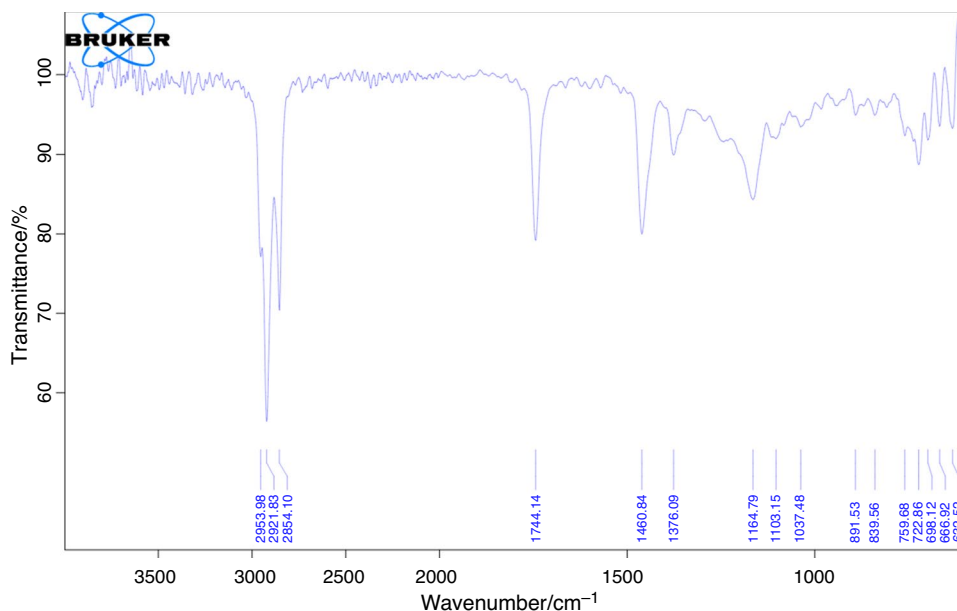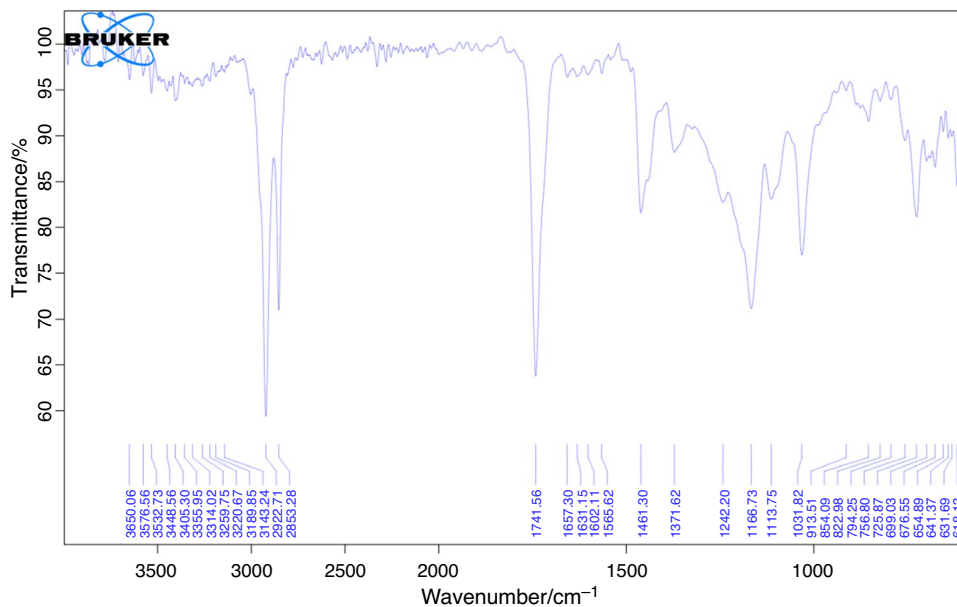**Fig. 7** Infrared spectroscopy of B40 FTIR

Fig. 8 Infrared spectroscopy of B100 FTIR

occurs from 260 to 380 °C, at which 9.30% mass reduced. At temperature 550.4 °C overall 98.12% mass reduced, while 1.88% mass residual. The B30 blend TG and DTG result present two mass loss steps. The preliminary mass loss occurs between 75 and 300 °C, during this 84.05% mass burnt, while second mass loss occurs from 300 to 380 °C, at which 9.30% mass reduced. At temperature 597.8 °C overall 99.98% mass reduced, while 0.02% mass residual. The thermogravimetric analysis of the B40 blend presents three mass loss steps from 100 to 600 °C, which occurs volatilization and combustion of triacylglycerides and burnt 98.31% mass of the sample. The first mass loss occurs between 100 and 330 °C, during this 79.96% mass burnt, second mass

loss occurs from 330 to 400 °C, at which 10.40% mass reduced, while third mass loss occurs from 400 to 600 °C, at which 7.86% mass burnt. At temperature 600 °C overall 98.31% mass reduced, while 1.69% mass residual. The B100 blend TG and DTG result present three mass loss steps. The first mass loss occurs between 160 and 360 °C, during this 50.45% mass burnt, the second mass loss step occurs from 360 to 540 °C, at which 44.82% mass reduced, while third mass loss occurs from 540 to 675 °C, at which 2.79% mass burnt. At temperature 675 °C overall 99.86% mass burnt, while 0.14% mass residual.
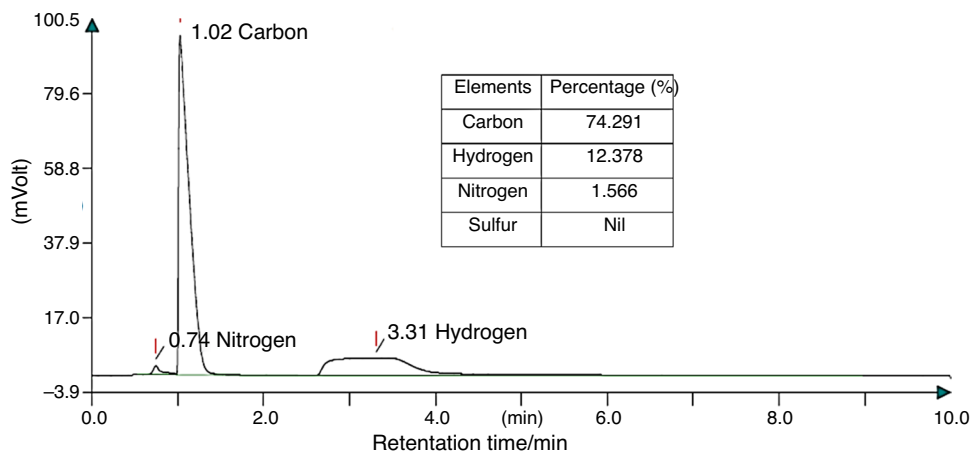
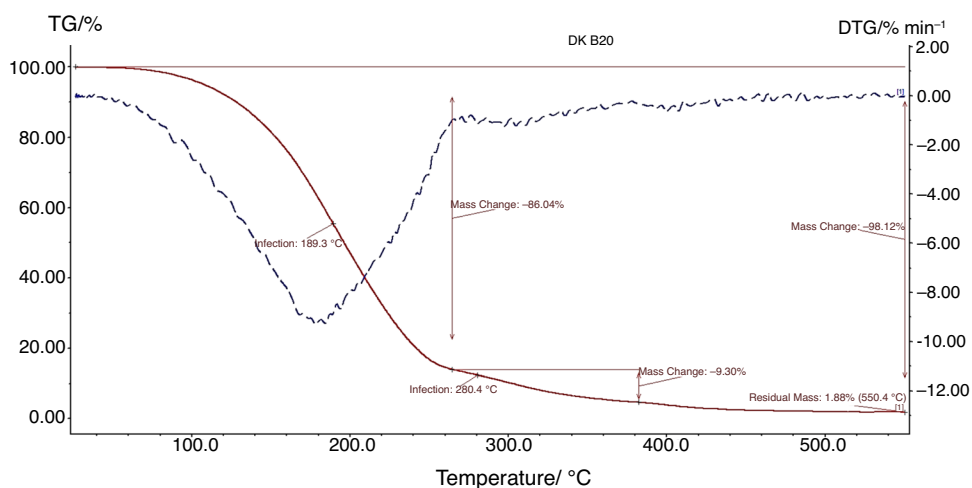**Fig. 9** CHNS composition of DK biodiesel

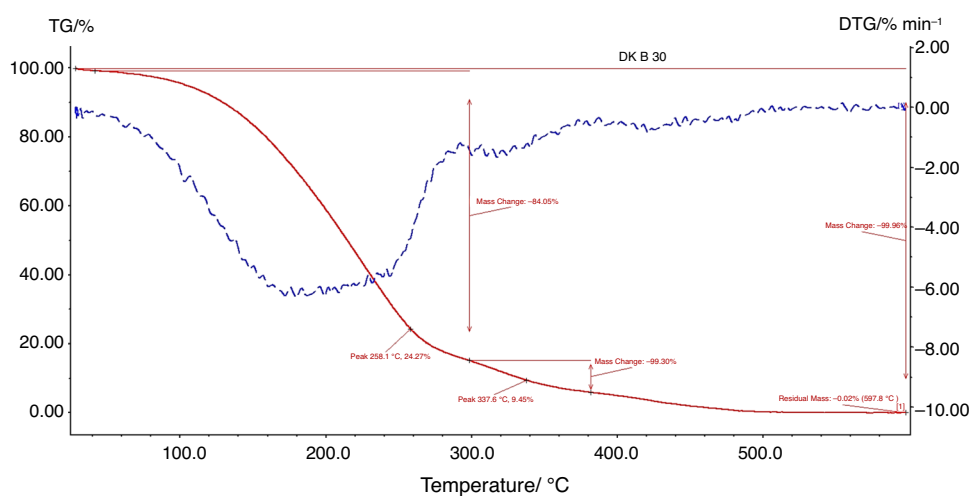**Fig. 10** B20 blend TG_DTG curve

Fig. 11 B30 blend TG_DTG curve

Fig. 12 B40 blend TG_DTG curve
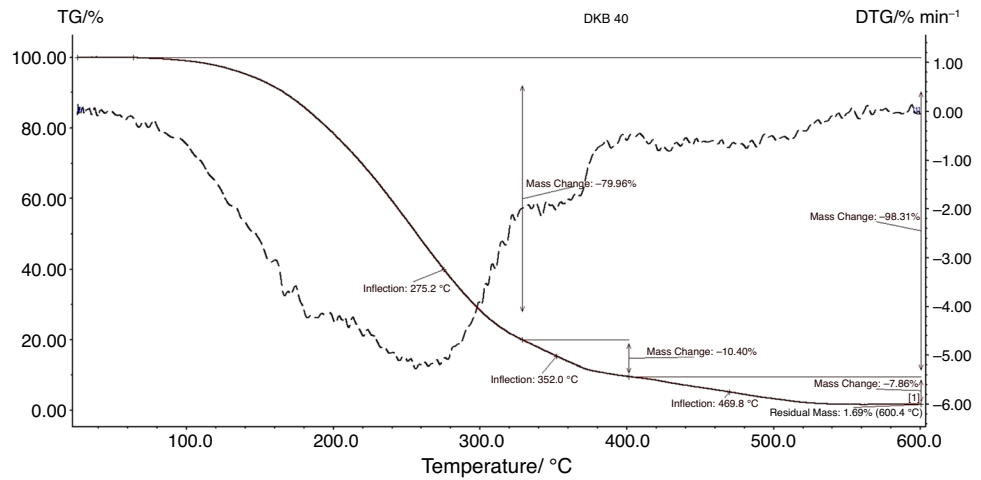
Fig. 13 B100 blend TG_DTG curve
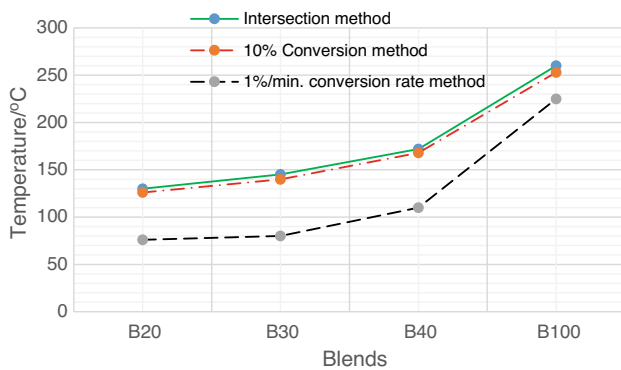
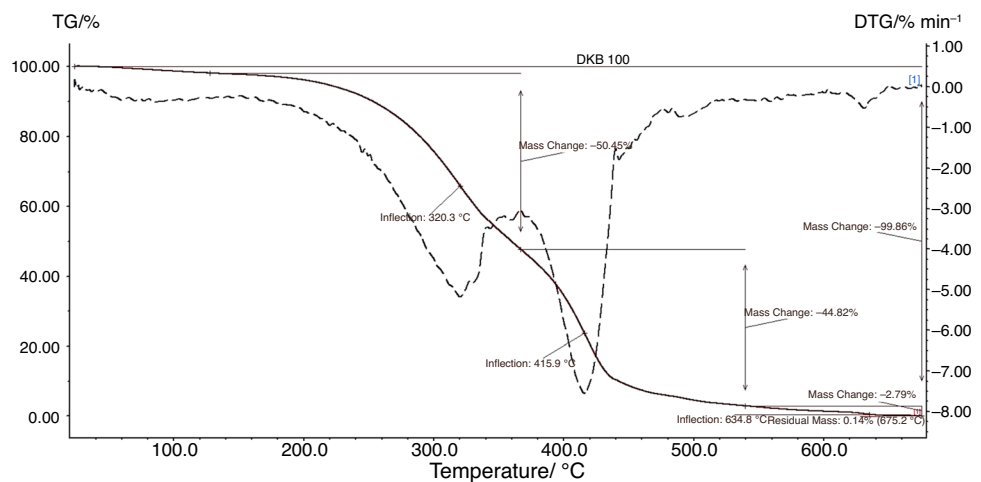**Fig. 14** Profile of ignition temperatures of blends as per different methods

Table 7 Ignition temperature of blends according to different methods

Blends	Intersection method	10% Conversion method	1% min^{-1} conversion rate method
B20	130	126	76
B30	145	140	80
B40	172	168	110
B100	260	253	225

Combustion characteristics

Figure 14 presents the profile of ignition temperatures of biodiesel blends using three discussed methods: (1) Intersection method (2) 10% conversion method (3) 1% min^{-1}

conversion rate method. The ignition temperature values are also given in Table 7. The 1% min^{-1} conversion rate method provides a lower value, while the intersection method provides a higher value of ignition temperature. The 10% conversion method provides the intermediate temperature as compared to the remaining methods. The pure biodiesel provides higher ignition temperature while the B20 blend provides lower ignition temperature.

The burnout temperature of blends was investigated using five different methods: (1) Intersection method (2)
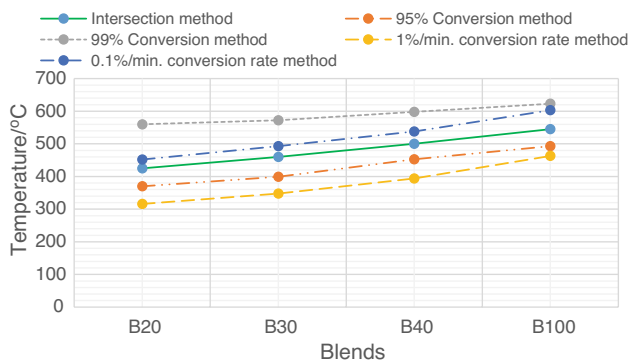
Fig. 15 Profile of burnout temperatures of blends as per different methods

Table 9 Thermogravimetry combustion data of biodiesel blend samples

Samples	Steps	T_i/°C	T_m/°C	T_f/°C	% of mass loss
B20	1st	65	180	260	86.04
	2nd	260		380	9.30
B30	1st	75	200	300	84.05
	2nd	300		380	9.30
B40	1st	100	260	330	79.96
	2nd	330		400	10.40
	3rd	400		600	7.86
B100	1st	160	320	360	50.45
	2nd	360		540	44.82
	3rd	540		675	2.79

95% conversion method (3) 99% conversion method (4) 1% min^{-1} conversion rate method (5) 0.1% min^{-1} conversion rate method. The burnout temperatures of biodiesel blends are presented in Fig. 15 and listed in Table 8. The 1% min^{-1} conversion rate method provides a lower value, while the 99% conversion method provides a higher value of burnout temperature. The remaining methods provide intermediate value of burnout temperature. The increasing percentage of biodiesel in the blend enhances the ignition, as well as burnout temperature of blends. The B20 blend shows lower burnout temperature as compared to remaining blends.

The thermogravimetry analysis also provides the initial temperature (T_i), maximum combustion rate temperature (T_m), and final decomposition temperature (T_f) of samples. Table 9 presents the mass loss steps of samples, initial, maximum combustion rate temperature, and final decomposition temperature with the percentage of mass loss. The increasing percentage of biodiesel in blend enhanced the onset decomposition temperature of blends. The B20 blend presents lower (65 °C), while B100 blend shows higher (100 °C) onset decomposing temperature. The several numbers of transitions are noticed in blends. The change in enthalpy with corresponding peak temperatures is listed in Table 10, and profile of energy changes according to temperature with transitions in blends is presented in Figs. 16–19.

The combustion characteristic results such as maximum combustion rate (DTG$_{max)}$, corresponding time required to

Table 10 Calorimetric data of biodiesel blend samples

Samples	Transition	T_{peak}/°C	Enthalpy change/J g^{-1}
B20	1st	232	145.308
	2nd	348	1617.76
	3rd	402	854.657
	4th	489	252.273
B30	1st	346	1289.65
	2nd	426	1133.32
	3rd	475	539.025
B40	1st	278	382.372
	2nd	368	2321.4
	3rd	430	934.898
	4th	480	1263.34
	5th	505	828.989
B100	1st	336	296.552
	2nd	416	1529.63
	3rd	464	466.463
	4th	495	1713.04
	5th	607	48.6948
	6th	610	44.3114
	7th	631	241.304

Table 8 Burnout temperature of blends according to different methods

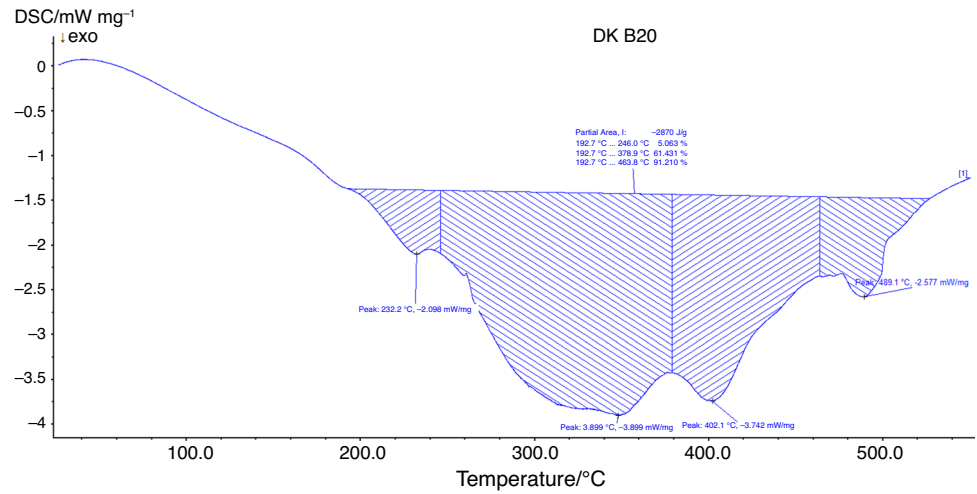| Blends	Intersection method	95% conversion method	99% conversion method	1% min^{-1} conversion rate method	0.1% min^{-1} conversion rate method
B20	425	370	560	316	452
B30	460	399	572	348	493
B40	500	453	598	394	538
B100	545	493	623	463	603

Fig. 16 B20 blend DSC analysis

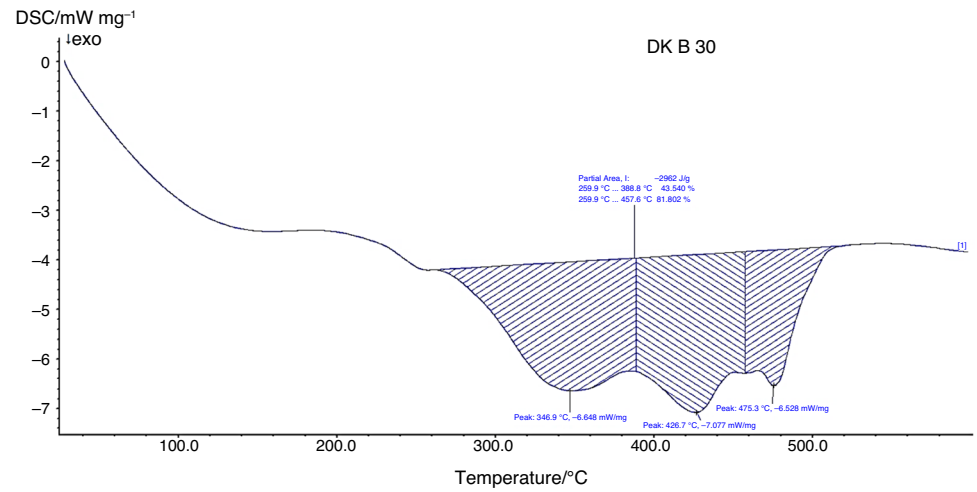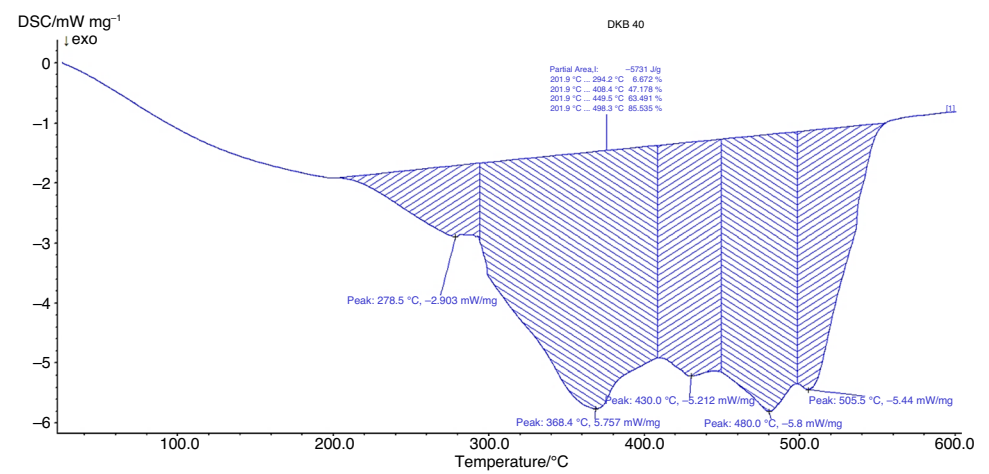

Fig. 17 B30 blend DSC analysis

Fig. 18 B40 blend DSC analysis

obtain maximum combustion rate (t_m), ignition index (Di), and comprehensive performance index (Dc) according to

different methods are presented in Table 11. The higher ignition index value of fuel provides the better ignition

performance during the combustion. According to results, the B20 blend provides the higher value of ignition index and it varies between 1.67×10^{-4} and 3.86×10^{-4} min^{-1} °C^{-2}. Likewise, the maximum comprehensive performance index delivers maximum active combustion. The B20 blend provides the higher value of comprehensive performance index, and it varies between 2.80×10^{-6} and 1.1×10^{-5} min^{-1} °C^{-3}.

Physicochemical properties

The physicochemical properties of biodiesel generated following IS1448 standards are compared with other biodiesels in Tables 12–15. The cetane number (a key parameter of fuel ignition) evaluated using Eq. (2) for DK biodiesel is 77.56. The ignition quality of fuel is defined by its cetane number. This high value of the cetane number will reduce the ignition delay period and minimize NOx emissions [28]. The viscosity of DK biodiesel is 7.03 mm^2 s^{-1}, which is high
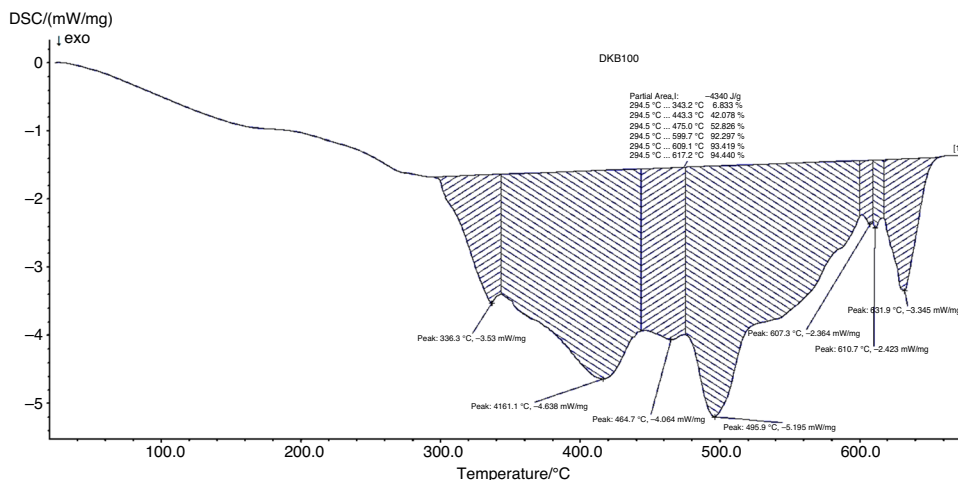
Fig. 19 B100 blend DSC analysis

Table 11 Combustion characteristics parameters of blends

Blends	DTG-$_{max}$/% min^{-1}	t_m/min	DTG-$_{mean}$/% min^{-1}	Intersection method		Conversion method		1% min^{-1} conversion rate method	
				Di/min^{-1} °C^{-2}	Dc/min^{-2} °C^{-3}	Di/min^{-1} °C^{-2}	Dc/min^{-2} °C^{-3}	Di/min^{-1} °C^{-2}	Dc/min^{-2} °C^{-3}
B20	9.26	14.95	2.17	1.67E−04	2.8E−06	1.99E−04	3.42E−06	3.86E−04	1.1E−05
B30	6.29	15.10	2.003	9.43E−05	1.3E−06	1.13E−04	1.61E−06	2.26E−04	5.66E−06
B40	5.26	22.72	1.78	6.12E−05	6.33E−07	6.91E−05	7.32E−07	1.21E−04	1.96E−06
B100	7.55	39.02	1.52	5.33E−05	3.11E−07	6.05E−05	3.64E−07	7.25E−05	4.9E−07

Table 12 DK biodiesel properties generated through IS1448 standards

Physicochemical properties	DK biodiesel	Standards specification		
		IS 1448	ASTM D6751	EN 14214
Cetane number	77.56	> 51	> 47	> 51
Density @ 15 °C/kg m^{-3}	890	860–900	880	860–900
Viscosity @ 40 °C/mm^2 s^{-1}	7.03	3.5–5.0	1.9–6.0	3.5–5.0
Acid number/mg KOH g^{-1}	1.8	0.5	0.5	0.5
Moisture content/mg kg^{-1}	Nil	500	500	500
Initial boiling point/°C	89	–	100–615	–
Flash point/°C	170	101	> 130	> 101
Fire point/°C	194	–	–	–
Pour point/°C	6	–	15–16	–
Cloud point/°C	19	–	3–12	–
Calorific value/MJ kg^{-1}	39.30	–	–	> 35

Table 13 Comparison of DK biodiesel with others

Biodiesels	Properties @ 40 °C	
	Density/kg m^{-3}	Viscosity/mm^2 s^{-1}
Rubber seed biodiesel [5, 29, 30, 43, 48–51]	860–897	3.7–8.02
Dairy waste scum [8, 52, 53]	860–875	3.8–4.2
Karanja oil biodiesel [10, 29, 54]	876–890	4.37–9.60
Camelina [16]	–	4.15
Caster biodiesel [16, 55]	947	10.22–14.82
Cuphea [16]	–	2.38
Pennycress [16]	–	5.24
Canola [16]	–	4.42
Soy [16]	–	3.95
Algae [16]	–	2.46
Polanga biodiesel [29, 43, 55]	874–910	4–5.70
Mohua biodiesel [29]	904–916	3.9–5.8
Jatropha curcus biodiesel [29]	864–880	3.7–5.8
Cotton seed biodiesel [29, 55]	874–911	2.2–4.9
Jojoba biodiesel [29]	863–866	19.2–25.4
Tobacco oil biodiesel [29]	860–888	3.5–4.23
Neem biodiesel [29]	860–965	5.2–48.5
Linseed oil biodiesel [29]	865–950	16.2– 36.6
Moringa Oleifera Biodiesel [29]	859.6	5.05
Waste fish oil biodiesel [55]	878	3.45
Mixed castor and waste fish oil [55]	898	3.61
Waste cooking oil biodiesel [56, 57]	870	6.09
DK biodiesel	890	7.03

when compared to that of diesel. This may due to the presence of fatty acids and the degree of saturation [1]. The high 170 °C flash point of DK biodiesel is good for storing and transportation. The viscosity and flash point can be reduced appropriately through additives for improving the quality of fuel and engine performance. The density of DK biodiesel is 890 kg m^{-3}, and its calorific value is 39.30 MJ kg^{-1}. The density of DK biodiesel is within the specified limits of IS standards. It is useful in judging the quality of ignition [46] and to complete the combustion of engine fuel [28]. The calorific value of fuel indicates the amount of energy emitted during combustion. The more amount of moisture content minimizes the calorific value of fuel and increases the density and viscosity of fuel [47]. The consumption of fuel is depending on its calorific value. The lower calorific value increases the requirement of fuel for the same work done. The calorific value of DK biodiesel has met the specifications of the standards. The moisture content is observed as

Table 14 Comparison of chemical properties of DK biodiesel with others

Biodiesels	Chemical properties			
	Cetane number	Acid number/mg KOH g^{-1}	Moisture/%	Calorific value/MJ kg^{-1}
Rubber seed biodiesel [5, 29, 30, 43, 48–51]	37–66.2	0.07–2.11	0.023–0.08	32.6–41.07
Dairy waste scum [8, 52, 53]	–	0.4–4.58	0.39	37.83–41.31
Karanja biodiesel [10, 29, 54]	38–60.9	0.72–0.76	–	36–39.69
Camelina [16]	52.8	–	–	–
Caster biodiesel [16, 55]	37–54.53	0.08	–	–
Cuphea [16]	56.1	–	–	–
Pennycress [16]	59.8	–	–	–
Canola [16]	55	–	–	–
Soy [16]	50	–	–	–
Algae [16]	36.5	–	–	–
Polanga biodiesel [29, 43, 55]	57.3–60	0.25	0.025	39.25–41.82
Tallow [16]	–	–	–	–
Mohua biodiesel [29]	51–52	–	–	39.4–39.91
Jatropha curcus biodiesel [29]	46–55	–	–	38.5–42
Cotton seed biodiesel [29, 55]	41– 59.5	0.16	–	39.5–40.1
Jojoba biodiesel [29]	63.5	–	–	42.76–47.38
Tobacco oil biodiesel [29]	49–51.6	–	–	38.43–39.81
Neem biodiesel [29]	51– 55.3	–	–	33.7–39.89
Linseed oil biodiesel [29]	28–35	–	–	37.7–39.8
Moringa Oleifera biodiesel [29]	56.3	–	–	40.05
Waste fish oil biodiesel [55]	55.59	0.10		–
Mixed castor and waste fish Oil [55]	56.97	0.06		–
Waste cooking oil biodiesel [56, 57]	57.03	0.36	–	37.47
DK biodiesel	77.56	1.8	Nil	39.30

Table 15 Comparison of cold flow properties of DK biodiesel with others

Biodiesels	Cold flow properties/°C		
	Flash point	Pour point	Cloud point
Rubber seed biodiesel [5, 29, 30, 43, 48–51]	110–184	− 8 to 4.8	− 6 to 5
Dairy waste scum [8, 52, 53]	105–142	− 8 to 3	− 2 to 9
Karanja biodiesel [10, 29, 54]	163–187	− 3 to 5.1	13–15
Camelina [16]	–	–	3
Caster biodiesel [16, 55]	158	< − 10	− 3
Cuphea [16]	–	–	− 9.1
Pennycress [16]	–	–	− 10
Polanga biodiesel [29, 43, 55]	151–187	4.3	13–16
Tallow [16]	–	–	17
Mohua biodiesel [29]	127–129	1–6	3–5
Jatropha curcus biodiesel [29]	163–238	5–6	10
Cotton seed biodiesel [29, 55]	120–243	− 15 to 6	1.7–7
Jojoba biodiesel [29]	61–75	− 6 to 6	6–16
Tobacco oil biodiesel [29]	152–165	− 12	–
Neem biodiesel [29]	34–165	4	8
Linseed oil biodiesel [29]	108	− 4 to − 18	1.7
Moringa Oleifera biodiesel [29]	150.5	19	19
Waste fish oil biodiesel [55]	96	− 1	3.0
Mixed castor and waste fish oil [55]	84	− 2	5.0
Waste cooking oil biodiesel [56, 57]	230	21	17
DK biodiesel	170	6	19

nil. The DK biodiesel has 1.8 mg KOH g^{-1} acid number, and its initial boiling point is 89 °C. The biodiesel shows a 19 °C cloud point and 6 °C pour point.

Conclusions

- Maximum 94% of FAME is recovered with methanol as alcohol, sulfuric acid (H$_2$SO$_4$) as a catalyst during esterification, potassium hydroxide (KOH) as a catalyst during transesterification along with 6:1 molar ratio, 1mass% catalyst concentration, 60 °C reaction temperature, 75-min reaction time.
- The DK biodiesel represents the presence of oleic acid, which is good for the balance of fuel in terms of ignition quality and viscosity.
- From infrared spectroscopy, it is seen that B20 blends illustrate similar and fewer vibration like diesel in different molecular bonds.
- The prepared DK sample possess 74.29% carbon, 1.566% nitrogen, 12% hydrogen, and 11.76% oxygen which satisfies the requirement of ASTM D6751 standards.
- As per emission acts, prepared DK sample is sulfur free, which restrict the sulfur oxide emissions.
- The TG–DTG results present the mass loss stages occurred during the combustion. The B20 and B30 blends present two mass loss steps, while B40 and B100 blends show more mass loss stages.
- The ignition temperature is investigated using three methods, while burnout temperature is investigated using five different methods. The increasing percentage of biodiesel in the blend enhances the ignition, as well as burnout temperature of blends. The B20 blend shows lower ignition and burnout temperature as compared to remaining blends.
- The B20 blend provides the higher value of ignition index, and it varies between 1.67×10^{-4} and 3.86×10^{-4} min^{-1} °C^{-2}. Likewise, the maximum comprehensive performance index delivers maximum active combustion. The B20 blend provides the higher value of comprehensive performance index, and it varies between 2.80×10^{-6} and 1.1×10^{-5} min^{-1} °C^{-3}.
- According to IS1448 standards, the DK biodiesel possesses good quality.
- The DK biodiesel presents high cetane number which is useful to improve ignition quality of blends. The higher value of the cetane number will reduce the ignition delay period and minimize NOx emissions.

Instrument Facility (SAIF), IIT Madras, Tamil Nadu-600036, India and Nirmala Innovations and Incubation Centre, Nirmala College of Pharmacy, Mangalagiri-522503, Andhra Pradesh, India for providing facilities to conduct experiments.

Funding This work is not supported fully or partially by any funding organization or agency.

Declarations

Conflict of interest The authors declare that there is no conflict of interests regarding the publication of this paper.

References

1. Ahmad J, Yusup S, Bokhari A, Kamil RNM. Study of fuel properties of rubber seed oil-based biodiesel. Energy Convers Manage. 2014;78:266–75. https://doi.org/10.1016/j.enconman.2013.10.056.
2. Sakthivel R, Ramesh K, Purnachandran R, Shameer PM. A review on the properties, performance and emission aspects of the third-generation biodiesels. Renew Sustain Energy Rev. 2017;82:2970–92. https://doi.org/10.1016/j.rser.2017.10.037.
3. Gülüm M, Bilgin A. Density, flash point and heating value variations of corn oil biodiesel-diesel fuel blends. Fuel Process Technol. 2015;134:456–64. https://doi.org/10.1016/j.fuproc.2015.02.026.
4. Ashok B, Nanthagopal K, Mohan A, Johny A, Tamilarasu A. comparative analysis on the effect of zinc oxide and ethanox as additives with biodiesel in CI engine. Energy. 2017;140:352–64. https://doi.org/10.1016/j.energy.2017.09.021.
5. Inggrid M, KristantoA SH. Optimization of transesterification of rubber seed oil using heterogeneous catalyst calcium oxide. AIP Conf Proc. 2015. https://doi.org/10.1063/1.4938308.
6. Atabani AE, Silitonga AS, Ong HC, Mahlia TMI, Masjuki HH, Badruddin IA, Fayaz H. Non-edible vegetable oils: a critical evaluation of oil extraction, fatty acid compositions, biodiesel production, characteristics, engine performance and emissions production. Renew Sustain Energy Rev. 2013;18:211–45. https://doi.org/10.1016/j.rser.2012.10.013.
7. Efthymiopoulos I, Hellier P, Ladommatos N, Profili AR, Eveleigh A, Aliev A, Kay A, Lamptey BM. Influence of solvent selection and extraction temperature on yield and composition of lipids extracted from spent coffee grounds. Ind Crops Prod. 2018;119:49–56. https://doi.org/10.1016/j.indcrop.2018.04.008.
8. Venkatesh BJ. Production of biodiesel from dairy wash water scum through heterogeneous catalyst and performance evaluation of tbc diesel engine for different diesel and methanol blend ratios. MTech. Thesis, Department of Thermal Power Engineering, Centre for Post Graduate Studies, Mysuru. Project:40S_B_MTECH_007. http://www.kscst.iisc.ernet.in/spp/40_series/SPP40S/03_Seminar_Biofuel_Projects/02_MTech_Projects/313_40S_B_MTECH_007.pdf
9. Watkins M, Nash D. Dairy factory wastewaters, their use on land and possible environmental impacts-a mini review. Open Agric. 2010;4:1–9.
10. Patel RL, Sankhavara CD. Biodiesel production from Karanja oil and its use in diesel engine: a Review. Renew Sustain Energy Rev. 2017;71:464–74. https://doi.org/10.1016/j.rser.2016.12.075.
11. Kumar MV, Babu AV, Kumar PR. Review the impacts on combustion, performance and emissions of biodiesel by using additives in direct injection diesel engine. Alex Eng J. 2018;57:509–16. https://doi.org/10.1016/j.aej.2016.12.016.
12. Shameer PM, Ramesh K, Sakthivel R, Purnachandran R. Biodiesel production through the use of different sources and characterization of oils and their esters as the substitute of diesel: a review. Renew Sustain Energy Rev. 2017;67:1267–81. https://doi.org/10.1016/j.rser.2016.09.117.
13. Singh SP, Singh D. Biodiesel production through the use of different sources and characterization of oils and their esters as the substitute of diesel: a review. Renew Sustain Energy Rev. 2010;14:200–16. https://doi.org/10.1016/j.rser.2009.07.017.
14. Atabani AE, Silitonga AS, Badruddin IA, Mahlia TMI, Masjuki HH, Mekhilef S. A comprehensive review on biodiesel as an alternative energy resource and its characteristics. Renew Sustain Energy Rev. 2012;16:2070–93. https://doi.org/10.1016/j.rser.2012.01.003.
15. Ghazali WNMW, Mamat R, Masjuki H, Najafi G. Effects of biodiesel from different feedstocks on engine performance and emissions: a review. Renew Sustain Energy Rev. 2015;51:585–602. https://doi.org/10.1016/j.rser.2015.06.031.
16. Knothe G, Razon LF. Biodiesel fuels. Prog Energy Combust Sci. 2017;58:36–59. https://doi.org/10.1016/j.pecs.2016.08.001.
17. Ferreira EN, Arruda TBMG, Rodrigues FEA, Arruda DTD, Júnior JHS, Porto DL, Ricardo NMSR. Investigation of the thermal degradation of the biolubricant through TGFTIR and characterization of the biodiesel-Pequi (Caryocar brasiliensis) as energetic raw material. Fuel. 2019;245:398–405. https://doi.org/10.1016/j.fuel.2019.02.006.
18. Zhou J, Xiong Y, Gong Y, Liu X. Analysis of the oxidative degradation of biodiesel blends using FTIR, UV–Vis, TGA and TDDES methods. Fuel. 2017;202:23–8. https://doi.org/10.1016/j.fuel.2017.04.032.
19. Marcelo YM, Leandro FC, Ricci TG, Viana LH, Oliveira SC, Junior AM, Oliveira LCS. Thermoanalytical methods in verifying the quality of biodiesel. Biofuels-Status Persp. 2015. https://doi.org/10.5772/59479.
20. Dweck J, Sampaio CMS. Analysis of the thermal decomposition of commercial vegetable oils in air by simultaneous TG/DTA. J Therm Anal Calorim. 2004;75:385–91. https://doi.org/10.1023/b:jtan.0000027124.96546.0f.
21. Candeia RA, Freitas JCO, Souza MAF, Conceicao MM, Santos IMG, Soledade LEB, Souza AG. Thermal and rheological behavior of diesel and methanol biodiesel blends. J Therm Anal Calorim. 2007;87:653–6. https://doi.org/10.1007/s10973-006-7861-2.
22. Santos NA, Tavares MLA, Rosenhaim R, Silva FC, Fernandes VJ, Santos IMG, Souza AG. Thermogravimetric and calorimetric evaluation of babassu biodiesel obtained by the methanol route. J Therm Anal Calorim. 2007;87:649–52. https://doi.org/10.1007/s10973-006-7765-1.
23. Souza AG, Danta HJ, Silva MCD, Santos IMG, Fernandes VJ, Sinfrônio FSM, Teixeira LSG, Novák CS. Thermal and kinetic evaluation of cotton oil biodiesel. J Therm Anal Calorim. 2007;90:945–9. https://doi.org/10.1007/s10973-006-8199-5.
24. Oliveira TF, Dweck J. Liquid phase oxidation quantitative analysis of biodiesel/diesel blends by differential TG and DTA. J Therm Anal Calorim. 2018;134:1953–63. https://doi.org/10.1007/s10973-018-7298-4.
25. Meireles RBRLA, Alcântara MA, Polari ILB, Santos AGSNA, Grisi CVB, Cordeiro AMTM. Catole coconut (Syagrus cearensis) oil: physicochemical characterization and thermo-oxidative stability by TG/DTG/DTA and Rancimat. J Therm Anal Calorim. 2021. https://doi.org/10.1007/s10973-021-10789-0.
26. Cortes MR, Queiroz JF, Santos TMN, Cavalheiro LF, Misutsu M, Ravaglia LM, Alcantara GB, Vian LH, Nazário CED, Simionatto E, Oliveira LCD. Applying quasi-isothermalthermogravimetry to determine degreesof oil conversion into biodiesel. J Therm Anal Calorim. 2021. https://doi.org/10.1007/s10973-021-10834-y.

27. Oliveira TP, Santos MFV, Batista ACM, Araújo AMM, Conceição MM, Fernandes VJ Jr, Gondim AD. CaO–TiO₂ bimetallic mixed oxideapplied to the production of biodiesel from cotton oil (Gossypium hisutum): monitoring of the procedure by TGA. J Therm Anal Calorim. 2021. https://doi.org/10.1007/s10973-021-10624-6.

28. More GV, Rao YVH. Biodiesel production with the help of different additives on the basis of standards-a Review. J Adv Res Dyn Control Syst. 2018;10:2050–64.

29. Onoji SE, Iyuke SE, Igbafe AI, Nkazi DB. Review: rubber seed oil: a potential renewable source of biodiesel for sustainable development in sub-Saharan Africa. Energy Convers Manage. 2016;110:125–34. https://doi.org/10.1016/j.enconman.2015.12.002.

30. Morshed M, Ferdous K, Khan MR, Mazumder MSI, Islam MA, Uddin MT. Rubber seed oil as a potential source for biodiesel production in Bangladesh. Fuel. 2011;90:2981–6. https://doi.org/10.1016/j.fuel.2011.05.020.

31. Krishnamurthy KN, Sridhara SN, Kumar CSA. Synthesis and optimization of Hydnocarpus wightiana and dairy waste scum as feedstock for biodiesel production by using response surface methodology. Energy. 2018;153:1073–86. https://doi.org/10.1016/j.energy.2018.04.068.

32. Yesilyurt MK, Cesur C. Biodiesel synthesis from Styrax officinalis L. seed oil as a novel and potential non-edible feedstock: a parametric optimization study through the Taguchi technique. Fuel. 2020;265:117025. https://doi.org/10.1016/j.fuel.2020.117025.

33. Ross PJ. Taguchi techniques for quality engineering. Singapore: McGraw-Hill; 1989.

34. Almazrouei M, Janajreh I. Thermogravimetric study of the combustion characteristics of biodiesel and petroleum diesel. J Therm Anal Calorim. 2019;136:925–35. https://doi.org/10.1007/s10973-018-7717-6.

35. Lu JJ, Chen WH. Investigation on the ignition and burnout temperatures of bamboo and sugarcane bagasse by thermogravimetric analysis. Appl Energy. 2015;160:49–57. https://doi.org/10.1016/j.apenergy.2015.09.026.

36. Peng C, Zhai Y, Zhu Y, Xu B, Wang T, Li C, Zeng G. Production of char from sewage sludge employing hydrothermal carbonization: char properties, combustion behavior and thermal characteristics. Fuel. 2016;176:110–8. https://doi.org/10.1016/j.fuel.2016.02.068.

37. Vamvuka D, Chatib NE, Sfakiotakis SI. Measurements of ignition point and combustion characteristics of biomass fuels and their blends with lignite. Proceedings of the European Combustion Meeting. 2011. https://www.researchgate.net/publication/232168026

38. Li XG, Lv Y, Ma BG, Jian SW, Tan HB. Thermogravimetric investigation on co-combustion characteristics of tobacco residue and high-ash anthracite coal. Biores Technol. 2011;102:9783–7. https://doi.org/10.1016/j.biortech.2011.07.117.

39. Ahn S, Choi G, Kim D. The effect of wood biomass blending with pulverized coal on combustion characteristics under oxy-fuel condition. Biomass Bioenerg. 2014;71:144–54. https://doi.org/10.1016/j.biombioe.2014.10.014.

40. Zhang B, Fu P, Liu Y, Yue F, Chen J, Zhou H, Zheng C. Investigation on the ignition, thermal acceleration and characteristic temperatures of coal char combustion. Appl Therm Eng. 2017;113:1303–12. https://doi.org/10.1016/j.applthermaleng.2016.11.103.

41. Shanab RAIA, Hwang JH, Cho Y, Min B, Jeon BH. Characterization of microalgal species isolated from fresh water bodies as a potential source for biodiesel production. Appl Energy. 2011;88:3300–6. https://doi.org/10.1016/j.apenergy.2011.01.060.

42. Bagul SY, Bharti KR, Dhar DW. Assessing biodiesel quality parameters for wastewater grown Chlorella sp. Water Sci Technol. 2017;76:719–27. https://doi.org/10.2166/wst.2017.223.

43. Roschat W, Siritanon T, Yoosuk B, Sudyoadsuk T, Promarak V. Rubber seed oil as potential non-edible feedstock for biodiesel production using heterogeneous catalyst in Thailand. Renew Energy. 2017;101:937–44. https://doi.org/10.1016/j.renene.2016.09.057.

44. Oyerinde AY, Bello EI. Use of fourier transformation infrared (FTIR) spectroscopy for analysis of functional groups in peanut oil biodiesel and its blends. Br J Appl Sci Technol. 2016;13(3):1–14. https://doi.org/10.9734/BJAST/2016/22178.

45. Hohn B. Haywood. Internal combustion engine fundamentals. 11th ed. McGraw Hill Education; 2015.

46. Fuels and Combustion. Bureau of energy efficiency. https://beeindia.gov.in/sites/default/files/2Ch1.pdf.

47. Hasannuddin AK, Yahya WJ, Sarah S, Ithnin AM, Syahrullail S, Sugeng DA, Razak IFA, Fatah AYA, Aqma WS, Rahman AHA, Ramlan NA. Performance, emissions and carbon deposit characteristics of diesel engine operating on emulsion fuel. Energy. 2018;142:496–506. https://doi.org/10.1016/j.energy.2017.10.044.

48. Gimbun J, Ali S, Kanwal CCSC, Shah LA, Ghazali NHM, Cheng CK, Nurdin S. Biodiesel production from rubber seed oil using a limestone based catalyst. Adv Mater Phys Chem. 2012;2:138–41. https://doi.org/10.4236/ampc.2012.24B036.

49. Krishnakumar U, Sivasubramanian V, Selvaraju N. Physico-chemical properties of the biodiesel extracted from rubber seed oil using solid metal oxide catalysts. Int J Eng Res Appl. 2013;3:2206–9.

50. Yang R, Su M, Zhang J, Jin F, Zha C, Li M, Hao X. Biodiesel production from rubber seed oil using poly (sodium acrylate) supporting NaOH as a water-resistant catalyst. Biores Technol. 2011;102:2665–71. https://doi.org/10.1016/j.biortech.2010.10.131.

51. Ahmad J, Yusup S, Bokhari A, Kamil RNM. Biodiesel Production from the high free fatty acid hevea brasiliensis and fuel properties characterization. Appl Mech Mater. 2014;625:897–900. https://doi.org/10.4028/www.scientific.net/AMM.625.897

52. Rahees K, Meera V. Production of biodiesel from dairy waste scum. Int J Sci Eng Res. 2014;5:194–9.

53. Yatish KV, Lalithamba HS, Suresh R, Arun SB, Kumar PV. Optimization of scum oil biodiesel production by using response surface methodology. Process Saf Environ Prot. 2016;102:667–72. https://doi.org/10.1016/j.psep.2016.05.026.

54. Sandeep G, Dattatreya G, Lakshmi SRS, Kumar NS, Venkatesh P. Karanja oil as an alternative fuel with air preheater. Int J Mech Eng Technol. 2017;8:218–25.

55. Fadhil AB, Tikrity ETBA, Albadree MA. Biodiesel production from mixed non-edible oils, castor seed oil and waste fish oil. Fuel. 2017;210:721–8. https://doi.org/10.1016/j.fuel.2017.09.009.

56. More GV, Koli SR, Rao YVH, Prasad PI, Rao BN. Effect of compression ratio on compression ignition engine with RUCO biodiesel/ diethyl ether/ diesel fuel blends. Energy sources, part a: recovery, utilization, and environmental effects. 2020. https://doi.org/10.1080/15567036.2020.1785593

57. Venkatesan K, Sathyaraj S. Performance and emission characteristics of cashew nut shell pyrolysed oil: waste cooking oil with diesel fuel in a four stoke di diesel engine. Int J Mech Prod Eng Res Dev. 2018;8:181–8.